Electronic Supporting Information (ESI)

Tunable LiCl@UiO-66 composites for water sorption-based heat transformation applications

Yangyang Sun,[a] Alex Spieß,[a] Christian Jansen,[a] Alexander Nuhnen,[a] Serkan Gökpinar,[a] Raphael Wiedey,[b] Sebastian-Johannes Ernst,[c] Christoph Janiak[a] *

[a] Institut für Anorganische Chemie und Strukturchemie, Heinrich-Heine-Universität Düsseldorf, 40204 Düsseldorf, Germany.

[b] Institut für Pharmazeutische Technologie und Biopharmazie, Heinrich-Heine-Universität Düsseldorf, 40204 Düsseldorf, Germany.

[c] Fraunhofer Institute for Solar Energy Systems (ISE), Heidenhofstr. 2, 79110 Freiburg, Germany.

Corresponding author: E-mail: janiak@uni-duesseldorf.de; Fax: + 49-211-81-12287; Tel: +49-211-81-12286

Additional email addresses:

Yangyang.Sun@uni-duesseldorf.de; alex.spiess@hhu.de; christian.jansen@hhu.de; alexander.nuhnen@uni-duesseldorf.de; serkan.goekpinar@uni-duesseldorf.de; mailto:raphael.wiedey@uni-duesseldorf.de; sebastian-johannes.ernst@ise.fraunhofer.de;

Principle of heat transformation processes

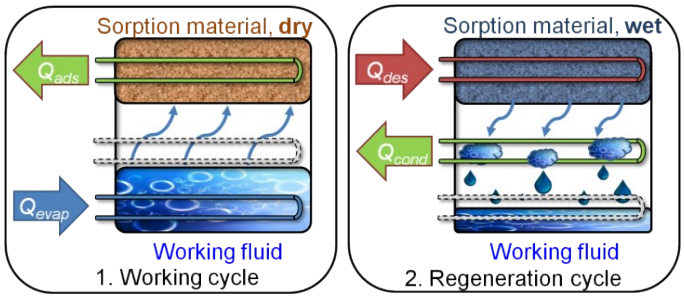

Fig. S1 In the working cycle, a working fluid (favorably water due to its high evaporation enthalpy and nontoxicity) is evaporated at a low pressure, taking up evaporation heat Q_{evap}. During incorporation into a porous material, heat of adsorption Q_{ads} is released. In the regeneration cycle, driving heat Q_{des} for desorption is applied, and further condensation takes place at a medium temperature level and releases condensation heat Q_{cond}. Depending on the operation direction, the device can be used as a chiller or a heat pump. Adapted from ref.[1] with permission from The Royal Society of Chemistry, copyright 2012.

Mechanism of water sorption for a CSPM

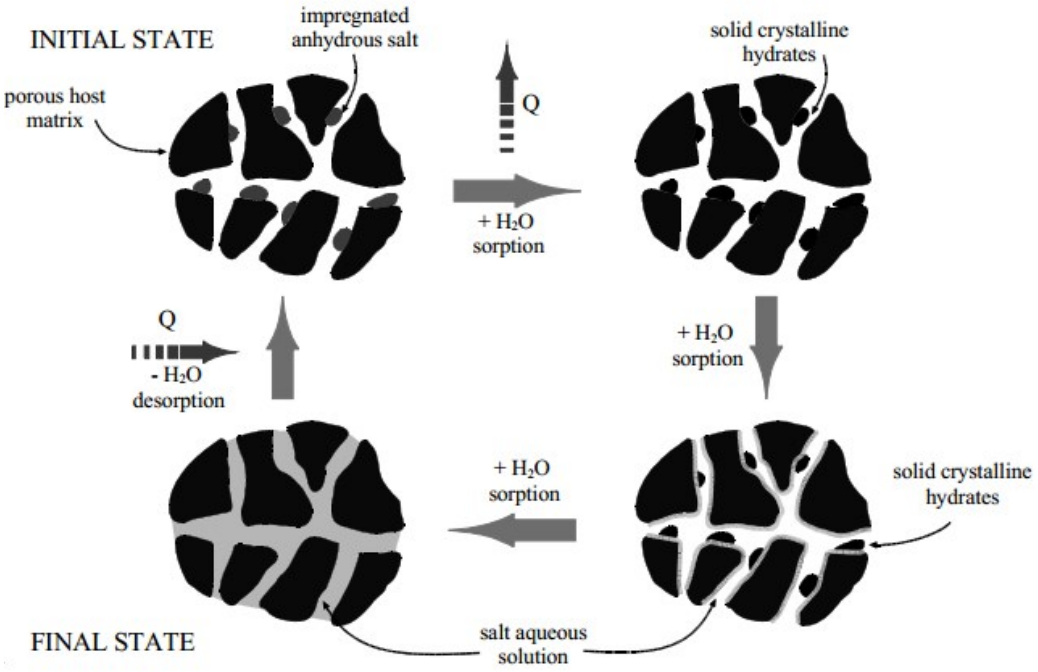

Fig. S2 Schematic presentation of the mechanistic aspects of water sorption of composite salts inside porous matrix (CSPM). Reprinted from ref.[2]. Copyright *Proc. VI Minsk International Seminar 'Heat Pipes, Heat Pumps, Refrigerators',* 2005.

Experimental scheme

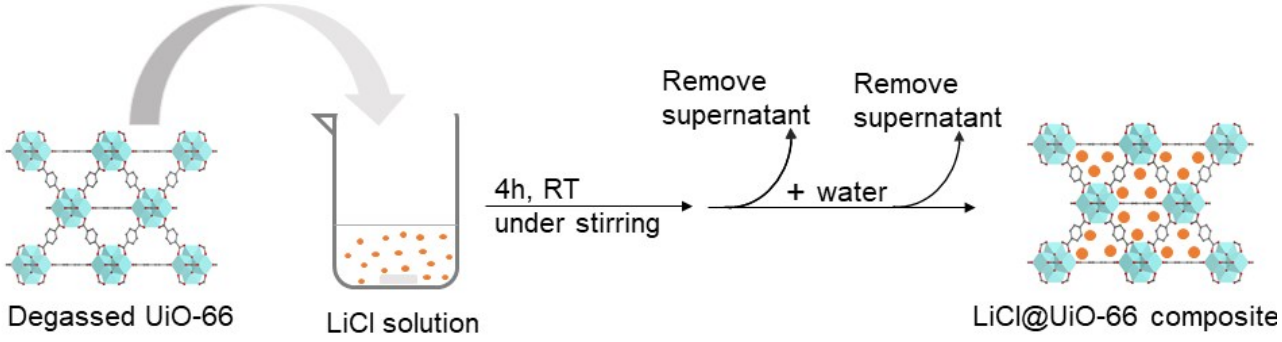

Scheme S1 Pictorial presentation of the work-flow to prepare LiCl@UiO-66 composite (CSPM) samples.

Solution preparation for atomic absorption spectroscopy (AAS)

The composites were outgassed at 150 °C under vacuum (0.05 mbar) for 2 h. Then a chosen amount (around 5 mg) of each composite was weighed with high accuracy into a 1.5 mL centrifuge tube (Eppendorf tube) and around 20 mg of CsF was added. Then two drops (0.1 mL) of 12 mol/L HCl and 1 mL of water were added. The dispersions were left standing overnight to achieve complete degradation. At last, the solutions were transferred to a 50 mL volumetric flask and water was added to the mark.

The mass fraction of m_{LiCl}/m_{CSPM} was calculated by Equations S1 and S2:

$$wt\%\left(m_{LiCl}/m_{CSPM}\right) = \frac{m_{LiCl}}{m_{CSPM}} = \frac{n_{LiCl} \times M_{LiCl}}{m_{CSPM}} \qquad \text{S1}$$

$$n_{LiCl} = \frac{c_{Li} \times V}{M_{Li}} \qquad \text{S2}$$

where:

m_{CSPM} refers to the used chosen mass of the CSPM composites. c_{Li} refers to the concentration of Li (mg/L), which was obtained from AAS analysis. V is the volume of the measured solution (50 mL). M_{Li} refers to the atomic mass of Li (6.941 g/mol). M_{LiCl} refers to the molar mass of LiCl (42.394 g/mol).

Scanning electron microscopy (SEM) and energy-dispersive X-ray spectroscopic (EDX) elemental mapping of CSPMs

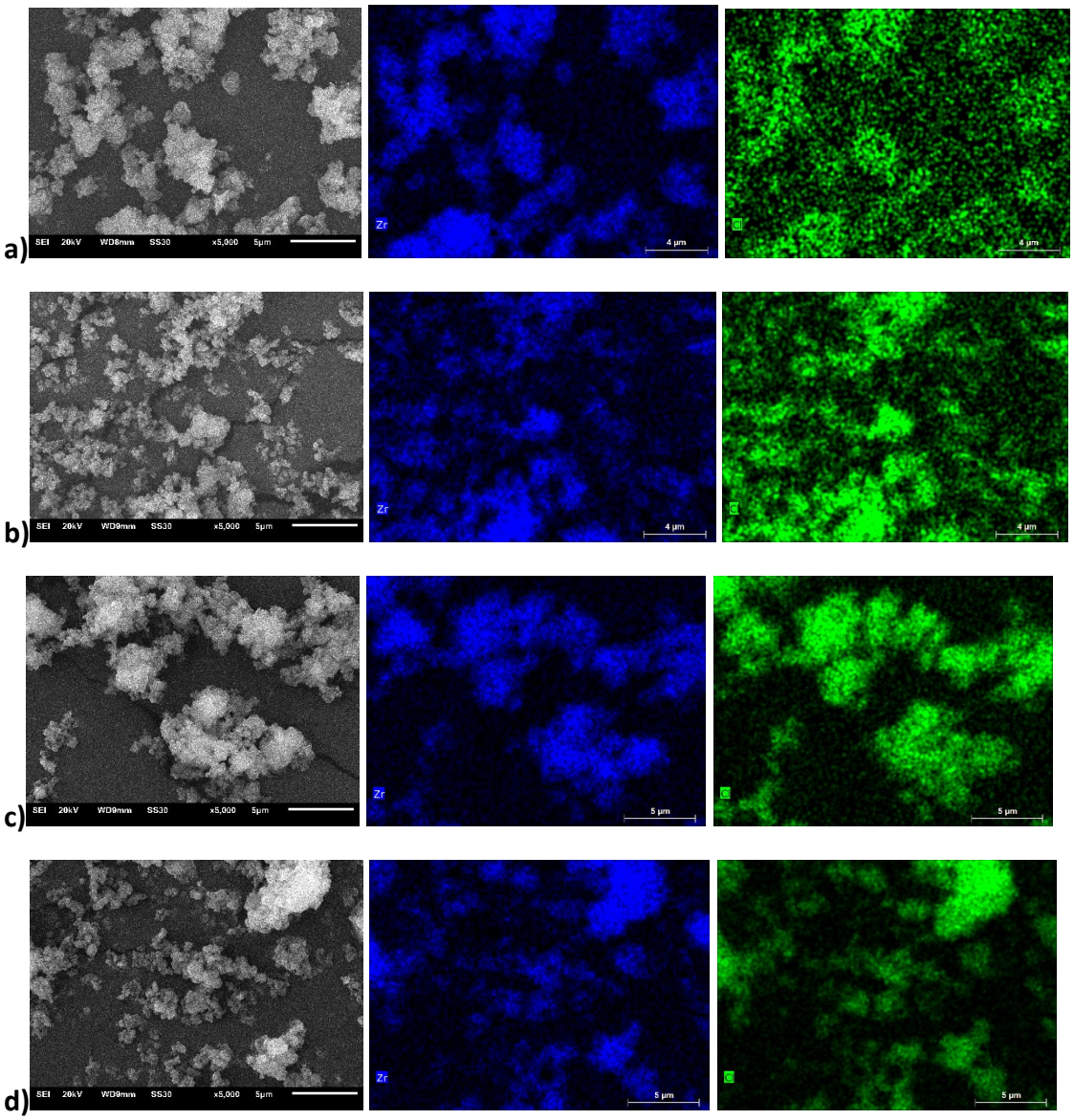

Fig. S3 SEM and EDX elemental mapping of zirconium (blue) and chloride (green) in (a) UiO-66 and (b-d) LiCl@UiO-66_x (x = 9, 19, 30) (top to bottom).

Determination of defects from thermogravimetric analysis (TGA)

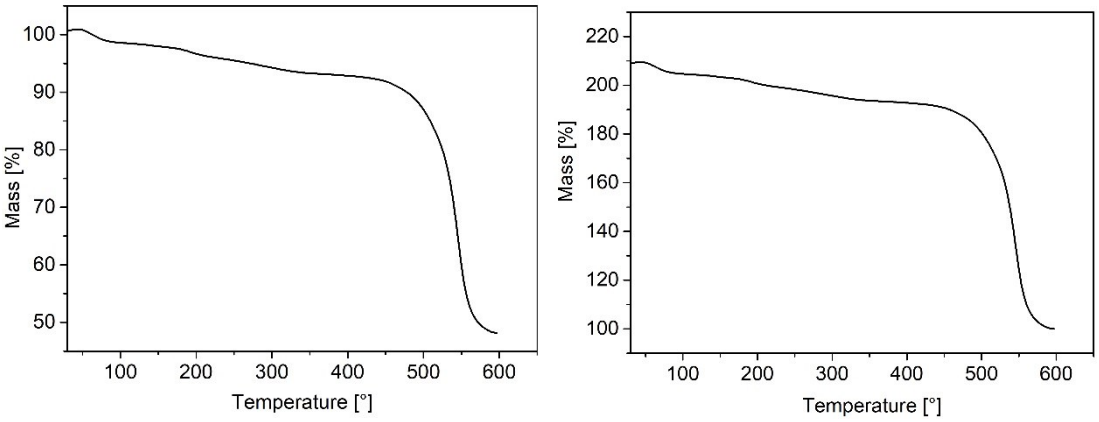

Fig. S4 TGA of UiO-66: normalized such that the initial weight = 100% (left) and normalized such that the final weight = 100% (right).

The solvent residues are removed under temperatures of 100 °C. The dehydroxylation of the $\{Zr_6O_4(OH)_4\}$ secondary building units (SBUs) appears in the temperature interval between 100 °C and 435 °C to yield $Zr_6O_6(BDC)_6$, followed by framework decomposition above 435 °C.

Determination of defects per SBU of UiO-66 was calculated with the assumption that the residue in TGA is pure ZrO_2 following the work of Shearer *et. al*.[3] The dehydroxylated ideal (defect-free) UiO-66 $Zr_6O_6(BDC)_6$ and its decomposition reaction would then be as follows:

$$Zr_6O_6(BDC)_6 + 45O_2 \rightarrow 6ZrO_2 + 48CO_2 + 12H_2O$$

The needed theoretical TGA plateau weight $W_{Theo.Plat.}$ and the theoretical weight contribution per BDC linker $Wt.PL_{Theo}$ was determined by Equation S3 and S4, respectively:

$$W_{Theo.Plat} = \left(\frac{M_{Comp.}}{M_{6 \times ZrO2}}\right) \times W_{End} \qquad \text{S3}$$

$$Wt.PL_{Theo} = \left(\frac{W_{Theo.Plat} - W_{End}}{NL_{Ideal}}\right) \qquad \text{S4}$$

where

M_{Comp} is the molar mass of dehydroxylated, defect-free UiO-66 $[Zr_6(\mu_3\text{-}O)(\mu_3\text{-}OH)_4(BDC)_6]$ (1628.03 g/mol).

M_{6xZrO2} is the molar mass of 6 moles of zirconium oxide (739.34 g/mol)

W_{End} is the end weight of the TGA run (100 % as normalized in the right part of Figure S2).

NL_{Ideal} is the number of linkers (6) in the ***ideal*** Zr_6 formula unit.

As a result,

$W_{Theo.Plat}$ for dehydroxylated UiO-66: **$W_{Theo.Plat}$** (UiO-66) = 220.20 %

$Wt.PL_{Theo}$ (UiO-66) = (220.20 – 100)/6 = 20.03 %

The experimental number of linkers per ***defective*** Zr_6-SBU, **NL_{Exp}** can be determined by Eq. S5:

$$NL_{Exp.} = (6 - x) = \frac{(W_{Exp.Plat} - W_{End})}{Wt.PL_{Thero}} \qquad \text{S5}$$

where

$W_{Exp.Plat}$ is the experimental TGA plateau and can be taken from the right part of Figure S2 (**$W_{Exp.Plat}$** = 192%).

x is the number of linker deficiencies per Zr_6 formula unit and can be determined by following equation:

$x = 6 - NL_{Exp} = 6 - [(W_{Exp.Plat} - W_{End})/Wt.PL_{Theo}]$= 6 – (192% – 100%)/20.03%

x = 1.4.

With **x** we obtain the experimental molecular weight Mw by using **$Zr_6O_{6+x}(BDC)_{6-x}$**

Mw (UiO-66) = 1427.10 g/mol

PXRD of recycled UiO-66 from LiCl@UiO-66_30

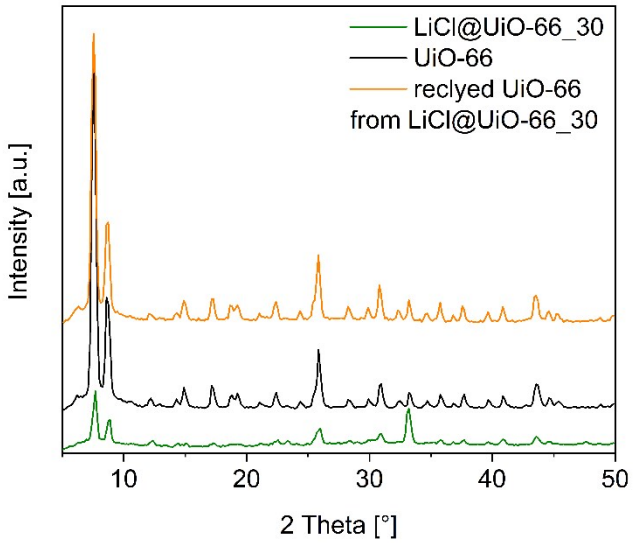

Fig. S5 PXRD patterns of UiO-66, LiCl@UiO-66_30 and recycled UiO-66 from LiCl@UiO-66_30. Recycled UiO-66 was regained by immersing LiCl@UiO-66_30 into methanol for 12 hours.

Water sorption isotherms

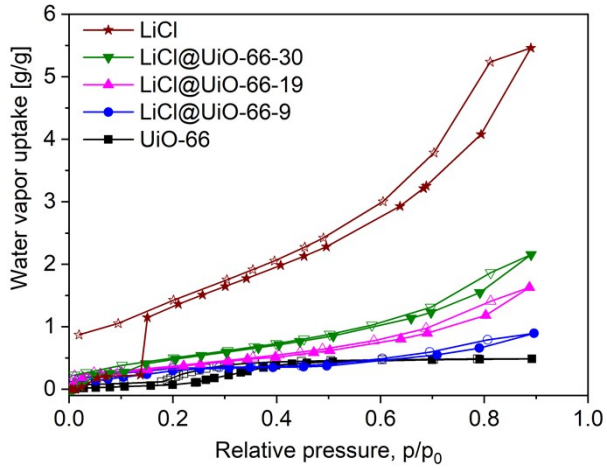

Fig. S6 Water sorption isotherms of neat LiCl, UiO-66 and LiCl@UiO-66_x, x = 9, 19, 30.

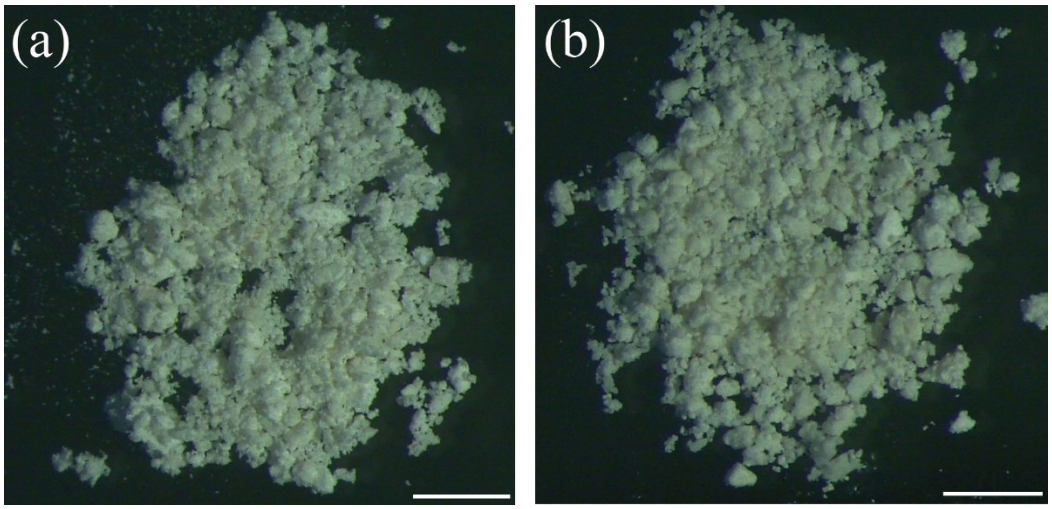

Fig. S7 Optical microscopy images of LiCl@UiO-66_30 (a) before and (b) after repeated water sorption with no drying procedure. The scale bar in both images is 0.5 mm.

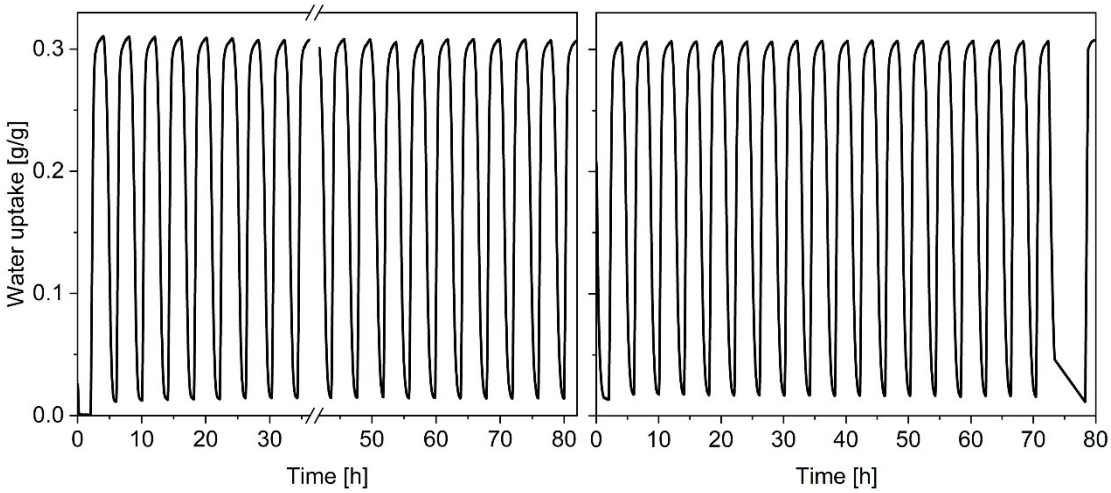
Water uptake [g/g]
0.0
0.1
0.2
0.3
0 10 20 30 50 60 70 80
Time [h]
0 10 20 30 40 50 60 70 80
Time [h]

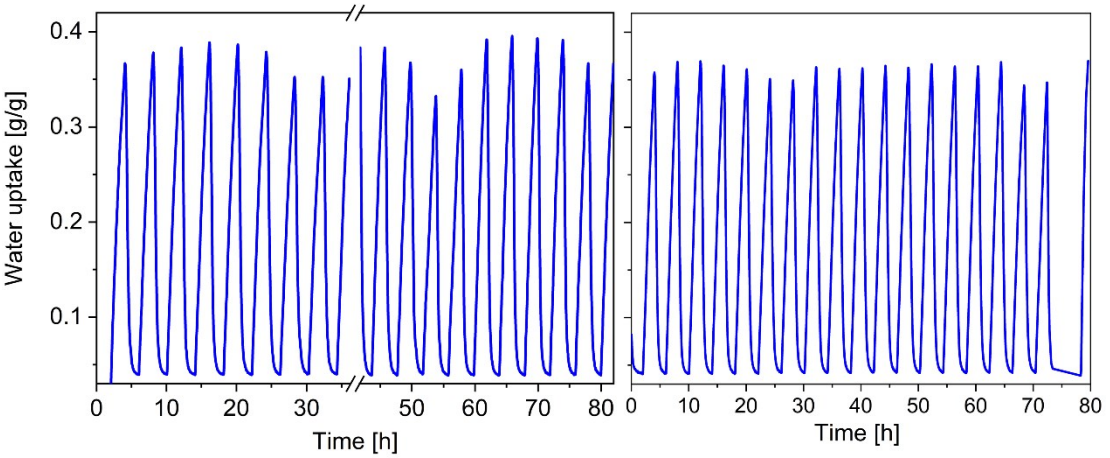
Water uptake [g/g]
0.1
0.2
0.3
0.4
0 10 20 30 50 60 70 80
Time [h]
0 10 20 30 40 50 60 70 80
Time [h]

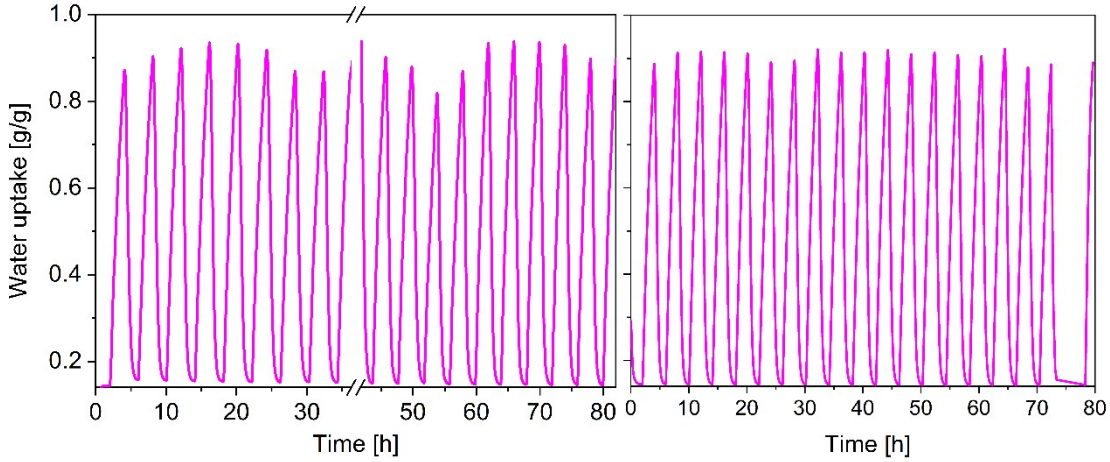
Water uptake [g/g]
0.2
0.4
0.6
0.8
1.0
0 10 20 30 50 60 70 80
Time [h]
0 10 20 30 40 50 60 70 80
Time [h]

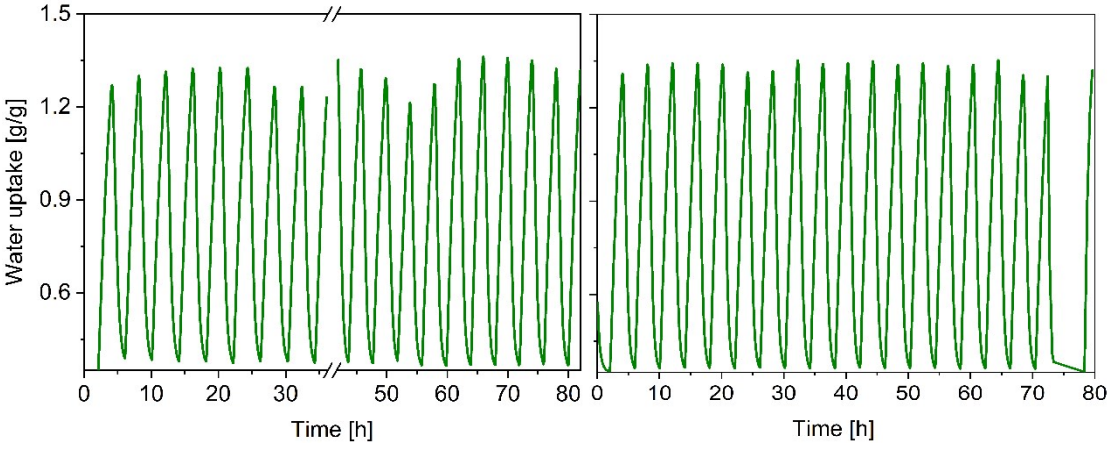
Water uptake [g/g]
0.6
0.9
1.2
1.5
0 10 20 30 50 60 70 80
Time [h]
0 10 20 30 40 50 60 70 80
Time [h]

Fig S8 Gravimetric adsorption and desorption cycles of UiO-66 (black) and the CSPMs LiCl@UiO-66_x, x= 9 (blue), 19 (pink), 30 (green) curve for first (left) and second (right) 20 cycles. The gravimetric multi-cycle tests were carried out between a relative humidity of 80% and 20% under a maximum equilibration time of 2 hours. The maximal number of cycles for the device is 20. When the first 20 cycles were finished, the instrument was restarted for the second 20 cycles with the sample remaining in the instrument. The data from 36 h to 42 h was excluded, as the sorption analyzer did not reach the targeted relative humidity during these hours.

Fitting curves for gravimetric water uptake over time

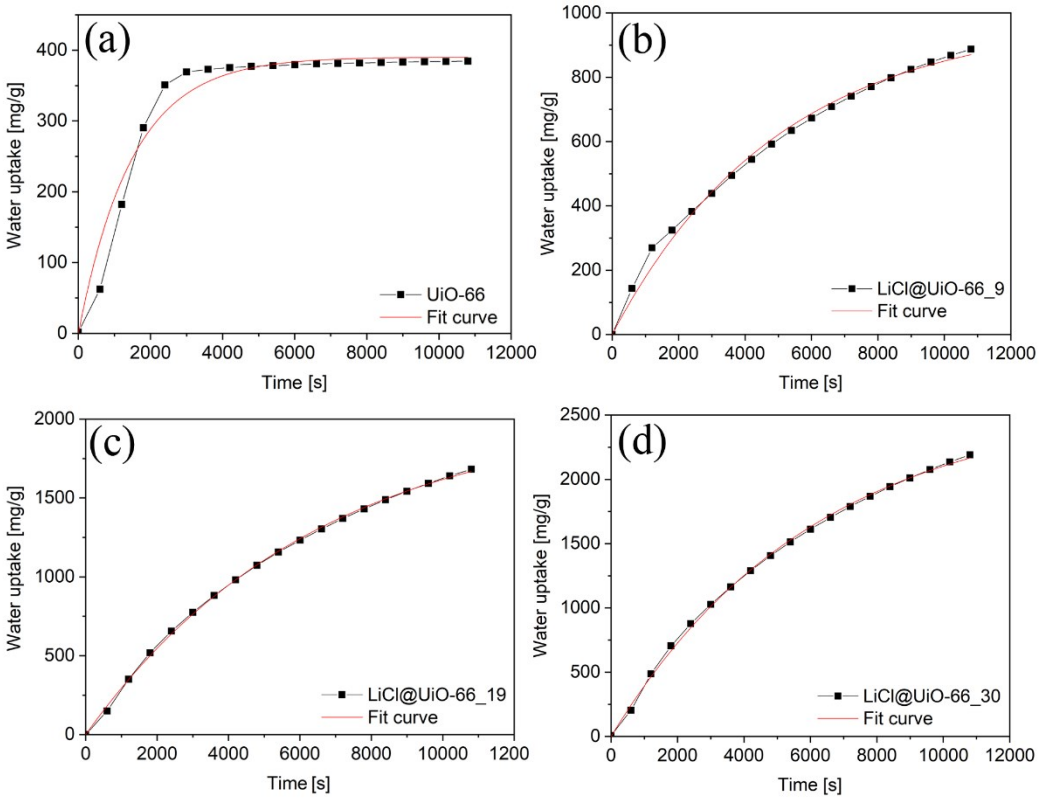

Fig. S9 Gravimetric water sorption measurements of UiO-66 and the CSPMs LiCl@UiO-66_x, x = 9, 19, 30 at 20 °C with corresponding fit curves using the BoxLucas1 model in Origin.

Coefficient of performance, COP calculation

To assess the potential of the "salt@MOF" adsorbent in adsorption heat transformation, the measured water adsorption data were transformed to the following equation according to the Dubinin-Astakhov approach, which is quite common for water@zeolite-systems.[4,5]

$$W(A) = W_0 exp\left[-(bA)^n\right] \quad \text{S6}$$

This approach defines an adsorbed volume W as $W = X/\rho_{H2O(liquid)}$ and an adsorption potential A as $A = -RTln\frac{p}{p_S(T)}$. The coefficients W_0, b, and n were fitted to experimental data.[6]

The coefficient of performance (COP) can be defined as the ratio of usable heat to spent heat:

$$COP = \frac{Q_{ads} + Q_{cond} + Q_{IC}}{Q_{des} + Q_{IH}} \quad \text{S7}$$

Herein in the numerator the usable heat is summed up (heat of adsorption (Q_{ads}), heat from condensation (Q_{cond}) and the heat from isosteric cooling (Q_{IC})). In the denominator the amounts of heat to apply for desorption (Q_{des}) and isosteric heating (Q_{IH}) of the adsorbent are summarized.

$$dQ_{IH} = m_{ads}(c_{p,ads} + X_{max}c_{p,fl})dT \quad \text{S8}$$

$$dQ_{des} = m_{ads}(c_{p,ads} + W(A)c_{p,fl})dT - m_{ads}q_{st}(T)dX \quad \text{S9}$$

$$dQ_{IC} = m_{ads}(c_{p,ads} + X_{min}c_{p,fl})dT \quad \text{S10}$$

$$dQ_{ads} = m_{ads}(c_{p,ads} + W(A)c_{p,fl})dT - m_{ads}q_{st}(T)dX \quad \text{S11}$$

$$Q_{cond} = m_{ads}\left(\Delta h_{cond}(T_{evap}) - c_{p,g}(\overline{T} - T_{cond})\right)(X_{max} - X_{min}) \quad \text{S12}$$

Herein m_{ads} refers to the adsorbent mass, $c_{p,ads}$, $c_{p,fl}$ and $c_{p,g}$ to the isobaric heat capacities of adsorbent, water and water vapor, $\overline{T}$ to the arithmetic mean temperature during desorption.

$$\overline{T} = 0.5(T_{des,max} + T_{des,min}) \quad \text{S13}$$

Using these set of equations, the COP for a heat pump cycle was calculated for a heating temperature of 40 °C, a cold temperature of 10 °C and a driving temperature of 90 °C. The capacity of the adsorbent $c_{p,ads}$ was assumed to 1 J/(g·K).

1 F. Jeremias, A. Khutia, S. K. Henninger and C. Janiak, *J. Mater. Chem.,* 2012, **22**, 10148-10151.

2 Yu. I. Aristov, An optimal sorbent for adsorption heat pumps: thermodynamic requirements and molecular design in *Proc. VI Minsk International Seminar 'Heat Pipes, Heat Pumps, Refrigerators',* Minsk, 12–15 September, 2005, 342–353.

3 G. C. Shearer, S. Chavan, S. Bordiga, S. Svelle, U. Olsbye and K. P. Lillerud, *Chem. Mater.*, 2016, **28**, 3749-3761.

4 L. X. Gong, R. Z. Wang, Z. Z. Xia and C. J. Chen, *J. Chem. Eng. Data*, 2010, **55**, 2920-2923.

5 X. Zheng, T. S. Ge, R. Z. Wang and L. M. Hu, *Chem. Eng. Sci.*, 2014, **120**, 1-9.

6 S.-J. Ernst, F. Jeremias, H.-J. Bart and S. K. Henninger, *Ind. Eng. Chem. Res.*, 2016, **55**, 13094-13101.